Endogenous LINE-1 (Long Interspersed Nuclear Element-1) Reverse Transcriptase Activity in Platelets Controls Translational Events Through RNA–DNA Hybrids

Hansjörg Schwertz, Jesse W. Rowley, Gerald G. Schumann, Ulrike Thorack, Robert A. Campbell, Bhanu Kanth Manne, Guy A. Zimmerman, Andrew S. Weyrich,* Matthew T. Rondina*

Objective—One source of endogenous reverse transcriptase (eRT) activity in nucleated cells is the LINE-1/L1 (long interspersed nuclear element-1), a non-LTR retrotransposon that is implicated in the regulation of gene expression. Nevertheless, the presence and function of eRT activity and LINE-1 in human platelets, an anucleate cell, has not previously been determined.

Approach and Results—We demonstrate that human and murine platelets possess robust eRT activity and identify the source as being LINE-1 ribonucleoprotein particles. Inhibition of eRT in vitro in isolated platelets from healthy individuals or in people with HIV treated with RT inhibitors enhanced global protein synthesis and platelet activation. If HIV patients were treated with reverse transcriptase inhibitor, we found that platelets from these patients had increased basal activation. We next discovered that eRT activity in platelets controlled the generation of RNA–DNA hybrids, which serve as translational repressors. Inhibition of platelet eRT lifted this RNA–DNA hybrid-induced translational block and was sufficient to increase protein expression of target RNAs identified by RNA–DNA hybrid immunoprecipitation.

Conclusions—Thus, we provide the first evidence that platelets possess L1-encoded eRT activity. We also demonstrate that platelet eRT activity regulates platelet hyperreactivity and thrombosis and controls RNA–DNA hybrid formation and identify that RNA–DNA hybrids function as a novel translational control mechanism in human platelets.

Visual Overview—An online visual overview is available for this article. (***Arterioscler Thromb Vasc Biol***. 2018;38:801-815. DOI: 10.1161/ATVBAHA.117.310552.)

Key Words: blood platelets ■ mice ■ platelet activation ■ retroelements ■ thrombosis

Megakaryocytes invest platelets with a complex transcriptome and requisite translational machinery including ribosomes, initiation and termination factors, microRNAs, and messenger RNAs (mRNAs).[1,2] Platelets use a variety of translational and posttranslational mechanisms to finely regulate their protein profile, although only some of these have been identified. For example, a subset of mRNAs are under the translational control of the mTOR pathway,[3,4] although this is thought to be mainly mRNAs possessing a 5′ terminal oligopyrimidine tract[5] or a pyrimidine-rich translational element.[6] An additional translational regulatory pathway in platelets is cytoplasmic, signal-dependent pre-mRNA splicing.[7,8] Nevertheless, only a limited number of pre-mRNAs have been identified in human platelets.[7–9] Therefore, additional translational control mechanisms likely exist in human platelets. Because of the anucleate nature of platelets, they serve as an ideal model system to study translational regulatory mechanisms.

See accompanying editorial on page 690

Because of their ability to insert themselves into various genomic locations, human transposable elements contribute importantly to a highly dynamic genome.[10] The only functional autonomous nonlong terminal repeat retrotransposon in humans is LINE-1 (long interspersed nuclear element-1, L1).[11] Almost 17% of the human genome consists of LINE-1 elements.[12,13] Active, full-length L1 elements consist of a 5′ untranslated region with internal promoter activity, 2 ORFs (open reading frames) separated by a short intergenic region, a 3′ untranslated region that ends with an AATAAA polyadenylation signal, and a poly(A) tail.[11,14,15] L1 mRNAs are atypical of mammalian mRNAs because they are bicistronic.[11] The 2 human ORFs in L1 elements (ORF1 and ORF2p [ORF2 proteins]) are in frame, separated by a 63-bp noncoding spacer that contains stop codons.[11] Translation of ORF1p (ORF1 protein) occurs via ribosomal initiation in the 5′ untranslated region,[16] whereas translation of ORF2p occurs

Nonstandard Abbreviations and Acronyms	
ART	antiretroviral therapy
eRT	endogenous reverse transcriptase
LINE-1	long interspersed nuclear element-1
MAP1LC3B	microtubule-associated protein 1 light chain 3 β
ORF	open reading frame
RNP	ribonucleoprotein –particle
RPL26	ribosomal protein L26
SELP	P-selectin

by an unconventional termination/reinitiation mechanism.[17] The COOH-terminal half of the 40-kDa ORF1p (p40) is involved in RNA binding and is well conserved across species.[11,18–20] ORF2 encodes an ≈150-kDa protein with 3 conserved domains: NH_2-terminal endonuclease domain, central reverse transcriptase (RT) domain, and COOH-terminal zinc finger-like domain.[11,21–23] Both L1-encoded proteins preferentially associate with their own encoding RNA (cis preference) to form a ribonucleoprotein particle (RNP) complex,[24,25] a proposed retrotransposition intermediate.[26,27] However, L1-encoded RT is also known to reverse transcribe RNAs encoded by *Alu* elements,[28] SVA elements,[29] and Pol II mRNAs causing processed pseudogene formation (26) in trans. L1 RT can reverse transcribe mRNAs coding for actin, GAPDH, and nucleolin into cDNAs.[30] In addition to shaping the genome over evolutionary time, L1 retrotransposition events alter gene expression patterns.[31] The most notable gene altering process involves insertional mutagenesis, which can serve as a functional gene knockout.[32] Retrotransposed L1 sequences can also function as alternative promoters that regulate gene transcription.[33] The insertion of L1 sequences into introns considerably reduces transcriptional elongation of target genes.[34] L1 retrotransposition events are responsible for diseases including hemophilia, β-thalassemia, and muscular dystrophy.[35] There is also evidence that endogenous RT (eRT) activity regulates cellular proliferation, differentiation, and gene expression.[36–41]

Reverse transcription of RNA also generates RNA–DNA hybrid intermediates. The formation of RNA–DNA hybrids has been used in molecular biology strategies as an in vitro technique to identify specifically translated mRNAs.[42,43] RNA–DNA hybrids also regulate transcriptional efficiency[44] and are required for efficient double-strand break repair.[45]

People with HIV are typically prescribed RT inhibitor–based therapy. The introduction of antiretroviral therapy (ART) has resulted in improved life expectancy.[46] However, people with HIV are at increased risk of thrombotic disorders, including atherothrombosis.[47–49] The molecular mechanisms underpinning this increased thrombosis risk remain unclear. In addition, whether platelets, which promote thrombosis, are directly affected by RT inhibitors has not been studied in detail. Accordingly, we sought to determine if human platelets possess RT activity and, if so, its functional effects.

Materials and Methods

Reagents and Antibodies

The following drugs and reagents were used freshly prepared or from stock solutions: nevirapine (100, 500, or 750 μmol/L in dimethyl sulfoxide [DMSO]; Sigma, St. Louis, MO). The following reagents and antibodies were used for microscopy, Western blot, and co-immunoprecipitation studies described below: paraformaldehyde (4% [2% final]), Alexa Fluor 546 conjugate of wheat germ agglutinin (1:1000; Life Technologies, Eugene, OR), custom rabbit anti-L1 ORF1p antibody #984 (provided by Schumann[29]), custom rabbit-anti-LINE-1 ORF2p (immunization peptide c+PKPGRDTTKKENFRP, 518–532, protein id AAD39215.1; Eurogentec, Liege, Belgium). This antibody was immunopurified and verified for specificity by Western blot (quench experiment). A rabbit anti-LINE-1 ORF2p and goat anti-P-selectin (Santa Cruz, TX), goat anti-T7, mouse anti-myc-DDK, rabbit anti-LC3B, and rabbit antiribosomal protein L26 (Abcam, Cambridge, MA), mouse anti-DNA–RNA hybrid (Kerafast, Boston, MA), rabbit anti-TAP (Thermo Fisher Scientific, Waltham, MA), Click-IT AHA (L-Azidohomoalanine), and Click-IT AF488 alkyne (1 mmol/L; Life Technologies).

Platelet Isolation and Culture

All studies were approved by the institutional ethics committee (IRB#000392 and IRB#00077138). Platelets used for the described studies were freshly isolated from medication-free, healthy human subjects or, in select studies, from patients with HIV (see below). Platelets were leukocyte reduced and isolated as previously described to yield a highly-purified population of cells with <1 leukocyte per 10× platelets.[7,8,50] Depleted platelets were resuspended at 1×10^8/mL in serum-free M199 medium, placed in round-bottom polypropylene tubes (Becton Dickinson, Franklin Lakes, NJ), and cultured in a 37°C humidified incubator at 5% CO_2 for different time points. In select studies, platelets were treated with nevirapine or its vehicle control (DMSO).

RT-Activity Assays

RT-activity assays were performed as previously described.[37] In brief, platelets (2×10^9/200 μL) or platelet-derived ribonucleoprotein particles (RNPs; see below for details) were lysed in a buffer containing 10 mmol/L Tris (2-amino-2-(hydroxymethyl)-1,3-propanediol)–HCl pH 7.5, 1 mmol/L MgCl₂, 1 mmol/L EGTA, 0.1 mmol/L PMSF (phenylmethane sulfonyl fluoride), 5 mmol/L β-mercaptoethanol, 0.5% CHAPS, and 10% glycerol. In select experiments, RNP lysates were immunodepleted for L1 ORF2p using the aforementioned anti-L1 ORF2p antibody and Agarose A/G plus beads (Life Technologies). The lysates were incubated on ice and finally centrifuged at 14 000 rpm for 30 minutes to remove any cell debris. In select experiments, the cell lysates were treated with nevirapine or its vehicle control (DMSO) or separated into retentate and filtrate using a 100 kDa spin column (EMD Millipore, Billerica, MA, according to the manufacturer's protocol). RT activity was tested using the ThermoScript reverse transcriptase polymerase chain reaction (RT-PCR) system (Life Technologies) in 20 μL reactions containing 10 ng of MS2 bacteriophage RNA (Roche Diagnostics, Basel, Swiss) or GFP (green fluorescent protein)-RNA (custom in vitro transcribed), which were treated with DNase, RT-PCR buffer, 5 mmol/L dithiothreitol, 1 mmol/L of 4 nucleotide triphosphate mix, 5 U of RNaseOUT, 15 pmol of MS2 reverse primer and substituting commercial RT with cell-free extract (1.5×10^7 total cell amount equivalent in each reaction). After the RT reaction, a 2 μL volume of the RT reaction were mixed with MS2 forward and reverse primers (5′-TCCTGCTCAACTTCCTGTCGAG-3′, 5′-CACAGGTCAAACCTCCTAGGAATG-3′), and polymerase chain reaction was performed using the ThermoScript RT-PCR kit (Life Technologies). To exclude non-specific amplification reaction or contamination we included a panel of positive and negative control reactions as previously described.[37] In vitro assays of RT inhibition were performed in the same mixtures as used for the RT activity assay except that the extracts were pre-incubated with various doses of non-nucleoside reverse transcriptase inhibitors (NNRTI) prior to adding the MS2 RNA template.

RNA Isolation

Platelets were lysed in TRIZOL, and RNA isolation was performed a previously described.[7,8]

Polymerase Chain Reaction and Real-Time Quantitative Polymerase Chain Reaction Studies

To determine LINE-1 mRNA expression pattern in human platelets, primers flanking ORF1 (5′-AGAAATGAGCAAAGCCTCCA-3′ and 5′-GCCTGGTGGTGACAAAATCT-3′) and ORF2 (5′-TCCAGCAG-CACATCAAAAAG-3′ and 5′-CCAGTTTTTGCCCATTCAGT-3′) were used (Figure 1C), and PCR was performed. PCR products were excised and subjected to Sanger Sequencing using standard methods. MAP1LC3B mRNA expression was detected by PCR and quantitative PCR (iCycler; BioRad, Hercules, CA) using the following primer set: 5′-GAAGTGGCTATCGCCAGAGT-3′ and 5′-GATTTTGGTTGGATGCTGCT-3′. RNA was detected using the following primer set: 5′-ATGGACCTTGGTGAATTGTGTG-3′ and 5′-TGGAAATGTGTCGTTCCTATGG-3′.

Platelet In Situ Hybridization Assays

For the assessment of in situ presence of LINE-1 mRNA and RNA in human platelets, platelets were fixed in suspension and spun down onto vectabond (Vector Laboratories, Burlingame, CA)-coated coverslips as previously described.[51] In situ hybridization was performed using custom-designed and manufactured probes (see schematic Figure 2D) against LINE-1 according to the manufacturer's algorithms and protocols (Biosearch Technologies, Novato, CA).

Immunocytochemistry

Freshly isolated platelets were fixed in suspension or placed in fibrinogen-coated chamber slides to induce platelet spreading at various times (2, 6, or 18 hours), fixed in paraformaldehyde, and subsequently incubated with IgG or an antibody against LINE-1 ORF1p or ORF2p (see the section on Reagents and Antibodies). In other experiments, platelets were either fixed immediately, to assess baseline RNA–DNA hybrid expression, or allowed to incubate for 18 hours in suspension. At the end of the experimental period, paraformaldehyde was added directly to the platelets to maintain the native morphology of the cells, as previously described.[8,50] Fixed platelets were subsequently layered onto vectabond (Vector Laboratories)-coated coverslips using a cytospin centrifuge (Shandon Cytospin; Thermo Fisher Scientific). Platelets were permeabilized, and RNA–DNA hybrids were specifically detected using the aforementioned antibodies. Specificity of the staining for anti–RNA-DNA hybrids was confirmed with isotype-matched nonimmune IgG. To further confirm the specificity of the staining procedure, we used differential digestion of RNAs (RNase I, RNase A [high NaCl], RNase A [low NaCl], and Turbo DNase, all from Life Technologies).

Protein Expression Studies

All samples were normalized for starting cell concentrations. Platelets or platelet-derived RNPs were lysed in Laemmli buffer, and samples were separated by SDS–PAGE and examined by Western analysis for LINE-1 ORF1p, and ORF2p expression patterns. Subsequently, proteins were detected by enhanced chemiluminescence. In quench experiments, the custom rabbit-anti-LINE-1 ORF2p antibody (see the section on Reagents and Antibodies) was preincubated with its corresponding immunogenic peptide to demonstrate specificity. Additionally, P-selectin, ribosomal protein L26, and MAP1LC3B were detected using the same technique. Quantification of Western blots was performed using ImageJ (National Institutes of Health).

Flow Cytometry

The expression of platelet surface adhesion molecules (eg, PAC-1 binding to activated integrin αIIbβ3) was evaluated by flow cytometry.[50] Freshly isolated platelets were cultured in the presence of nevirapine 750 µmol/L or its vehicle (DMSO, 6 hours), and subsequently activated with thrombin (0.1 U/mL) for 10 minutes (Figure 4B). For Figure 4E, baseline platelets from healthy individuals and persons positive for HIV were evaluated. The cells were incubated with fluorescein isothiocyanate–conjugated antibody PAC-1 (number: 340535;

BD Biosciences), fixed, and analyzed on a 5-color FACScan analyzer (BD Biosciences) with appropriate isotype controls. Samples were analyzed using FlowJo v9 (Flowjo LLC, Ashland, OR).

In Vivo Pulmonary Embolism Model

All animal studies were approved by the University of Utah IACUC (protocol 15-10004). Eight- to 12-week-old male and female mice C57Bl/6 mice were either administered 150 mg/kg nevirapine resuspended in saline with 0.2% methylcellulose or vehicle control (saline with 0.2% methylcellulose) by oral gauge once a day for 4 consecutive days. On the fifth day, mice we subjected to a collagen/epinephrine pulmonary embolism model as previously described.[52] Cessation of breathing was monitored for 10 minutes before animals were euthanized by CO_2 asphyxiation.

RNP Isolation

RNP isolation was performed according to the study by Kulpa et al.[30] In brief, platelets were lysed in RNP lysis buffer (1.5 mmol/L KCl, 2.5 mmol/L $MgCl_2$, 5 mmol/L Tris–HCl [pH 7.4], 1% [w/v] deoxycholic acid, 1% [v/v] Triton X-100, and 1× Complete Mini EDTA-free protease inhibitor cocktail [Roche Diagnostics]). Cleared supernatant was layered onto a sucrose cushion (8.5% and 17% [w/v] sucrose in 80 mmol/L NaCl, 5 mmol/L $MgCl_2$, 20 mmol/L Tris–HCl [ph 7.5], 1 mmol/L dithiothreitol, and 1× Complete Mini EDTA-free protease inhibitor cocktail). After a centrifugation step of 178000g for 2 hours, the resulting pellet was lysed in TRIZOL for RNA isolation or in RT-activity assay buffer to assess for RT activity.

In Vitro Translation of ORF1p and RNA Binding and Immunoprecipitation Studies

We first in vitro translated ORF1p. In brief, a T7 promoter was put in front of the ORF1p coding segment of the pAD2TE plasmid (provided by J.V. Moran[53]) by using a PCR approach (T7 LINE-1 ORF1 forward 5′-TAATACGACTCACTATAGGGATGGGGAAAAAACAGAACAG -3′, T7 LINE-1 ORF1 reverse 5′- TTAACCCATTTGCTGTCCA CCAGTCATGCTAGC -3′). The resulting PCR product was in vitro transcribed using the MEGAscript T7 kit, supplemented with the anti-reverse cap analog, and poly(A)-tailed using a poly(A)-tailing kit (all from Life Technologies). RNA was subsequently isolated and introduced into the 1-step human coupled IVT kit (Thermo Fisher Scientific) according to the manufacturer's protocol. For all RNA binding and immunoprecipitation (IP; RIP) studies, the Magna RIP RNA-binding protein immunoprecipitation kit (EMD Millipore) was used according to the manufacturer's protocol. In brief, in vitro translated T7-tagged ORF1p was used in each reaction (specific antibody and the isotype-matched nonimmune IgG). The magnetic beads used for the IP reaction were prepared by incubating the beads with the antibody of interest (goat anti-T7; Abcam) or the respective IgG control for 30 nutes at room temperature. IP was performed using the prepared beads, the supplied buffer, and the in vitro translated T7-tagged ORF1p with constant rotation overnight at 4°C. After several washes, total RNA (1.5 µg/sample) was isolated from platelets, added to the bead-bound protein, and incubated overnight at 4°C under constant rotation. Finally, beads were pelleted, and RNA bound to ORF1p was isolated using TRIZOL according to the manufacturer's protocol. For cDNA synthesis, the superscript II RT-PCR system (Life Technologies) was used. After the RT reaction, a 2 µL volume of the RT reaction was mixed with ORF2 primer (5′-TCCAGCAG-CACATCAAAAAG-3′ and 5′-CCAGTTTTTGCCCATTCAGT-3′), or MAP1LC3B primer (5′-GAAGTGGCTATCGCCAGAGT-3′ and 5′-GATTTTGGTTGGATGCTGCT-3′), and PCR was performed.

Analysis of Platelet Morphology

For assessment of extended platelets with ≥2 cell bodies, platelets were isolated and resuspended at 1×10^8 mL in serum-free M199 medium and cultured in a 37°C humidified incubator at 5% CO_2 for 6 hours in the presence of nevirapine or its vehicle (DMSO). The time

course for these experiments was selected based on published studies from our laboratory identifying that 6 hours allows for extended cell body formation ex vivo.[50] After the incubation period, cells were carefully fixed (paraformaldehyde) and spun on glass coverslips. Random fields (3 for each experimental condition) were recorded using microscopy techniques. Total platelets per field were counted (average 450 cells/field). Extended platelets were defined as platelets clearly possessing an extended morphology and ≥2 distinct cell bodies as previously described by our group and others.[50,54] Changes in the formation of extended platelets were analyzed and compared with vehicle-treated conditions.

Protein De Novo Synthesis Studies

Microscopy-based global protein synthesis studies using Click-IT AHA (L-Azidohomoalanine) were performed as previously described.[50] For these studies, an average of 1000 platelets per treatment arm were analyzed using CellProfiler software (see below for details). For global protein synthesis studies using radioactively labeled amino acids, purified platelets were resuspended at 1×10^8/mL in serum-, methionine-, and cysteine-free DMEM (Life Technologies), placed in round-bottom polypropylene tubes (Becton Dickinson), and cultured overnight in a 37°C humidified incubator at 5% CO_2 in the presence of [^{35}S]methionine and [^{35}S]cysteine. In select studies, platelets were treated with nevirapine or vehicle control (DMSO). Two-dimensional gel electrophoresis was performed as previously described.[50] In brief, platelets were lysed in buffer containing 7 mol/L urea, 2 mol/L thiourea, 4% CHAPS (3-[(3-cholamidopropyl)dimethylammonio]-1-propanesulfonate), 40 mmol/L TRIS (base), and 2 tablets of a protease inhibitor mix per 20 mL of buffer stock solution (complete mini; Roche Diagnostics). Isoelectric focusing was performed using the Protean IEF Cell (BioRad) at a temperature of 20°C. Gel strips (pH 3–10L; GE Healthcare, Marlborough, MA) were rehydrated for 12 hours at 50 V using a buffer containing 7 mol/L urea, 2 mol/L thiourea, 2% CHAPS, 0.5% IPG buffer (pH 3–10L), dithiothreitol (2.8 mg/mL), and traces of bromophenol blue. The samples were applied as part of the rehydration solution, and lysates were run on a 11-cm strip (linear gradient for 2 hours (100 V), linear gradient for 1 hour (500 V), linear gradient for 5 hours (1000 V), linear gradient for 2.5 hours (8000 V), and then a quick ramp and hold for 35 minutes (8000 V). For the second dimension (SDS–PAGE), IPG strips were equilibrated for 20 minutes in buffer (6 mol/L urea, 30% v/v glycerol [87% v/v], 2% w/v SDS, 50 mmol/L Tris–Cl, pH 8.8, 100-mg dithiothreitol/10 mL, and traces of bromophenol blue). Gels (4–20%; Jule, Milford, CT) were coomassie stained using an optimized protocol from Neuhoff et al[55,56] and subsequently dried and exposed to a Biomax MR film (Carestream, Rochester, NY) for autoradiographic detection.

RNA–DNA Hybrid Immunoprecipitation Studies (Modified RIP)

For all modified RIP studies, the Magna RIP RNA-binding protein immunoprecipitation kit (EMD Millipore) was used according to the manufacturer's protocol. In brief, 24×10^9 total platelets were first lysed in 200 μL of complete RIP lysis buffer. Next, 12×10^9 platelets were used in each reaction for the hybrid-specific antibody and the isotype-matched nonimmune IgG. The magnetic beads used for the IP reaction were prepared by incubating the beads with the antibody of interest (anti-RNA–DNA hybrid) or the respective IgG control for 30 minutes at RT. RIP was performed using the prepared beads, the supplied buffer, and 100 μL of the platelet cell lysate with constant rotation for 4 hours at 4°C. Phenol-chloroform isolation techniques were used for RNA purification with an additional overnight ethanol precipitation step. RNA yield was measured using the NanoDrop spectrometer. RNA–DNA hybrids were stored at −80°C until sequencing was performed.

Next-Generation RNA Sequencing

The cDNA libraries for deep sequencing were prepared using random hexamers. Samples were sequenced using the NEBNext Multiples Small RNA library Prep Set kit for 50 cycles as single reads, sequencing version 4, on an HiSeq sequencer, and sequence reads were processed and aligned to hg38 as previously described.[57,58]

Translational Block Experiments

The translational block experiments were based on the RT-activity assay described above. In brief, platelets (2×10^9/200 μL) were lysed in the RT buffer. The platelet lysate was preincubated with nevirapine (500 μmol/L for 45 minutes at 37°C) with and without a melting step (2 minutes at 95°C) to separate RNA–DNA hybrids. The RT activity assay was set up in 20 μL reactions containing 70.8 ng of MAP1LC3B in vitro–transcribed mRNA (True ORF RC207356; Origene, Rockville, MD; mMESSAGE mMACHINE T7 Ultra Kit, Life Technologies), which was DNase treated. After the RT reaction, the resulting nucleic acids were introduced into an in vitro translation assay (1-step human coupled IVT kit; ThermoFisher Scientific, Waltham, MA). The resulting myc-DDK tagged MAP1LC3B protein was separated by SDS–PAGE and examined by Western analysis for myc-DDK-tagged MAP1LC3B expression. Quantification of Western blots was performed using ImageJ (NIH).

Studies in Patients With HIV

All studies were approved by the institutional ethics committe (IRB#00077138). Platelets used for the described studies were freshly isolated as described above from consenting patients with HIV. Patients were excluded if taking immunosuppressant medications, had concurrent infection with hepatitis C, or another acute viral or bacterial infection, for which they were actively being treated or had been treated in the last 4 weeks.

Infection Studies

DENV2 was propagated in C6/36 *Aedes albopictus* mosquito cells[59] and titrated by plaque assay on LCC-MK2 cells. The amount of infectious particles was expressed as plaque-forming units per milliliter. Supernatants from uninfected cell cultures (mock) were produced using the same conditions. Freshly isolated platelets (multiplicity of infection 0.2) were infected with DENV2 and incubated for 24 hours with the virus before being analyzed.

Laser Capture Microscopy

Resting-state human platelets were isolated and fixed in suspension (see above). Platelets were spun down on a membrane slide (PEN membrane glass slide; Thermo Fisher Scientific). The samples were dehydrated using increasing ethanol concentrations and a final incubation step in xylene for 5 minutes. For laser capture microscopy, we used a Veritas system (Arcturus Bioscience, MountainView, CA). The laser power of the cutting laser was set to 2.28, the capture laser was set at 70 mA, pulse length 2000 μsec, and a frequency of 10 hits. Membrane pieces were captured in macro laser capture microscopy caps (Thermo Fisher Scientific). RNA from target cells was isolated using the PicoPure RNA isolation kit (Thermo Fisher Scientific) and subsequently amplified using the RiboAmp HS PLUS Kit (Thermo Fisher Scientific). cDNA synthesis and PCR for LINE-1 ORF1 and ORF2 were performed as described above.

Microscopy and Image Analysis

Fluorescence microscopy and high-resolution confocal reflection microscopy was performed using an Olympus IX81, FV300 (Olympus, Melville, NY) confocal-scanning microscope equipped with a 60×/1.42 NA oil objective for viewing platelets. An Olympus FVS-PSU/IX2-UCB camera and scanning unit and Olympus Fluoview FV 300 image acquisition software version 5.0 were used for recording. In addition, an EVOS FL Auto Cell imaging system with integrated dual camera system, system-specific software and equipped with a 60×/1.42 NA oil objective was used. Monochrome 16-bit images were further analyzed and changes quantified using Adobe Photoshop CS6, ImageJ (NIH), and CellProfiler (www.cellprofiler.org).[60,61]
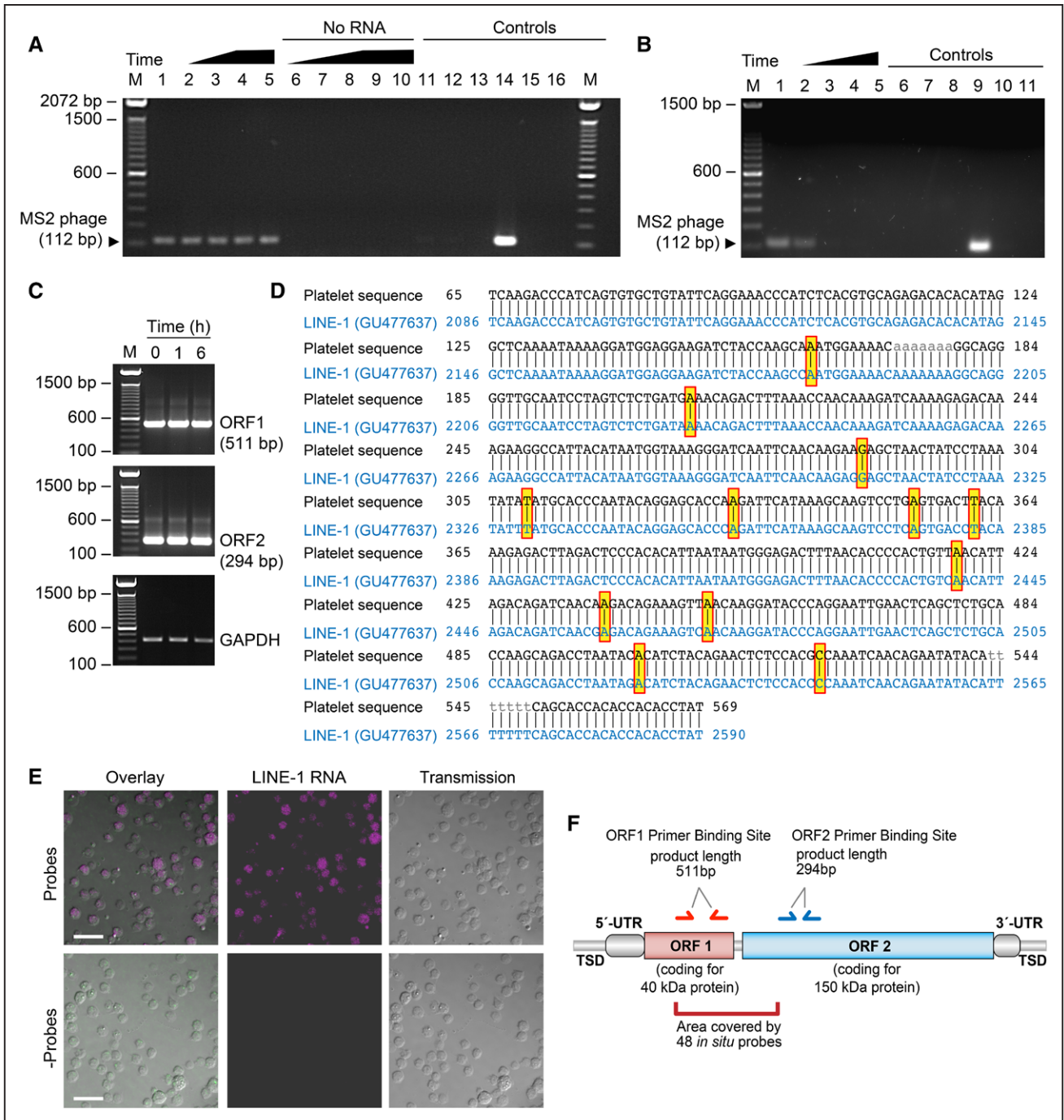
Figure 1. Human platelets possess endogenous reverse transcriptase (RT) activity and express LINE-1 (long interspersed nuclear element-1) *ORF1* (open reading frame) and *ORF2* mRNA. **A**, Platelet lysates were incubated with (lanes 1–5) or without (lanes 6–10) exogenous MS2 phage RNA. Lanes 11 to 16 represent controls. The following conditions apply: Lanes 1, 6—freshly isolated platelets; lanes 2,7—platelets stored for 2 h; lanes 3, 8—platelets stored for 4 h; lanes 4, 9—platelets stored for 6 h; lanes 5, 10—platelets activated with thrombin (0.1 U/mL) for 6 h; lane 11—platelet lysate replaced with the lysis buffer only; lane 12—omission of the platelet lysate; lane 13—omission of the MS2 phage RNA; lane 14—platelet lysate replaced with commercial RT; lane 15—omission of the reverse MS2 phage primer; lane 16—negative PCR. This figure is representative of n>10 independent experiments. **B**, Platelets were treated with DMSO (Veh, lane 1) or increasing concentrations of nevirapine ([26 µg/mL], [130 µg/mL], and [195 µg/mL], lanes 2–4, respectively), and reverse transcription of exogenous MS2 phage RNA was measured. Controls include lane 5—no RNA; lane 6—platelet lysate replaced with the lysis buffer only; lane 7—omission of the platelet lysate; lane 8—omission of the platelet lysate and MS2 phage RNA; lane 9—platelet lysate replaced with commercial reverse transcriptase (RT); lane 10—omission of the reverse MS2 phage primer; lane 11—negative PCR. This figure is representative of 5 independent experiments. **C**, Freshly isolated platelets were examined at baseline (*t*=0 h) or stimulated with thrombin (0.1 U/mL) for 1 or 6 h. RNA from the platelets was isolated and *ORF1* and *ORF2* mRNA expression was evaluated by PCR. **Bottom**, *GAPDH* as a loading control. This figure is representative of 3 independent experiments. **D**, PCR products for LINE-1 were excised and sequenced using Sanger sequencing. The resulting sequence was aligned with a reference sequence. Yellow boxes highlight mismatches. **E**, Human platelets were fixed in suspension and Stellaris FISH probes specific for LINE-1 (magenta, **top**) were hybridized to detect *LINE-1* mRNA in situ. **Bottom**, Platelets where the probes were omitted (–Probes) as a control (scale bars=10 µm). (*Continued*)

Statistical Analyses

The mean±SEM was determined for each variable. Student 2-tailed *t* tests or ANOVA was used to identify differences among 2 or multiple experimental groups, respectively. If significant differences were found, a Newman–Keuls post-hoc procedure was used to determine the location of the difference. A 2-tailed *P* value <0.05 was considered significant.

Results

ERT Activity Is Present in Human Platelets

Although in nucleated cells endogenous retrotransposon-encoded RT (eRT) is essential for the mobilization of transposable elements, eRT activity has not previously been examined in human platelets. Therefore, we first determined whether human platelets possess eRT activity using a PCR-based in vitro assay.[37] An exogenous MS2 phage RNA is added to isolated platelet lysates, and evidence of reverse transcription is detected by probing for the DNA product of MS2 phage. We found that eRT activity is present in platelets at baseline and is retained over time (Figure 1A). Stimulating platelets with thrombin (*t*=6 hours) did not visibly alter eRT activity (Figure 1A, lane 5). In parallel experiments, we also confirmed that platelets in vitro transcribe an exogenously added GFP RNA, thus excluding the possibility of contaminating bacteria which are used to produce MS2 phage RNA[62] in the PCR reagents (data not shown). Treating platelets with nevirapine, a clinically used RT inhibitor, blocked reverse transcription of exogenous MS2 phage in a dose-dependent manner (Figure 1B). Additional experiments of platelet lysates with 100 kDa size exclusion–based spin columns (Figure I in the online-only Data Supplement) suggested that LINE-1 elements could account for most of the eRT activity (ie, fully processed HERV-K RT has an MW of 66 kDa).

Human Platelets Express LINE-1 ORF1 and ORF2

Human platelets express mRNA encoding LINE-1 ORF1 and L1 ORF2 (Figure 1C and 1D). Activation of platelets did not visibly alter the expression of LINE-1 ORF1 or ORF2 (Figure 1C). We next performed in situ hybridization experiments using custom-designed probes against LINE-1 (Figure 1E). The specificity of the in situ experiments is based on the ability to detect a visible signal only if multiple probes align with their target RNA sequentially (mismatches indicated in Figure 1D are most likely artifacts introduced during the sequencing process). Consistent with our findings by PCR and Sanger sequencing (Figure 1C and 1D), we found that *LINE-1* mRNA is endogenously expressed in situ in the cytoplasm of unstimulated human platelets (Figure 1E, see also Figure 1F demonstrating binding sites of primer pairs and in situ probes). Laser capture microscopy of individual human platelets further confirmed LINE-1 *ORF1* and *ORF2* expression (Figure II in the online-only Data Supplement). Laser capture microscopy also excludes the possibility that signals

detected in the PCR experiments are derived from LINE-1 mRNA or DNA introduced by contaminating nucleated cells.

We next investigated the localization of LINE-1 encoded ORF1 (ORF1p) and ORF2p in human platelets. Both ORF1p and ORF2p are robustly expressed basally in the cytoplasm of unstimulated platelets (Figure 2A). In activated platelets, LINE-1 proteins concentrated and accumulated in the middle of the cell bodies (Figure 2A, arrows), cellular regions rich in mRNAs and ribosomal constituents.[7,8] LINE-1 proteins were also detected in megakaryocytes and proplatelet extensions (data not shown). When platelets were allowed to culture overnight (18 hours), ORF2p continued to be robustly expressed and was also identified in the cytoplasm of platelets with extended cell bodies[50,54] (Figure III in the online-only Data Supplement). Immunoblotting also demonstrated that ORF1p (Figure 2B) and ORF2p (Figure 2C) proteins were present in platelets. Specificity of the anti-ORF2p antibody was confirmed by performing a quench experiment using the immunogenic peptide (Figure 2C).

Platelets Contain RNPs Harboring L1 mRNA and L1 ORF2p

We hypothesized that RNPs in platelets contain functional LINE-1 mRNA and LINE-1 ORF2p harboring reverse transcriptase activity. Therefore, to further identify the localization and function of endogenous L1-encoded RT (eRT) in platelets, we focused on the subcellular localization of eRT. RNPs are intracellular complexes integral to the regulation of gene expression.[63] To examine whether the eRT expression and activity we identified (Figures 1 and 2) is contained within RNPs, we next determined whether RNPs isolated from platelets harbored reverse transcriptase activity. Purified RNPs from platelets were sufficient to reverse transcribe an exogenous MS2 phage RNA in an in vitro RT activity assay (Figure 3A), indicating that platelet eRT activity is found within RNPs. We next investigated whether the eRT activity is ORF2p (which contains the RT domain) dependent. RNP lysates used for RT activity assays were depleted of LINE-1 ORF2p using the anti-ORF2p antibody characterized in Figure 2. Immunodepletion of LINE-1 ORF2p reduced RT activity by >60% (Figure 3B), indicating that the LINE-1 ORF2p RT domain is the major source for platelet eRT. Consistent with the eRT activity associated with RNPs, RNA coding for LINE-1 ORF1 and ORF2 was identified within isolated platelet RNPs (Figure 3C). Furthermore, L1 ORF2p was confirmed in platelet-derived RNPs (Figure 3D). To confirm that platelets are capable of forming L1 RNPs, we in vitro translated T7-tagged ORF1p using the plasmid pAD2TE1[27] as a template. Next, isolated total platelet RNA was incubated with the recombinant T7-tagged ORF1p, and ORF1p-bound RNA was subsequently immunoprecipitated using the T7 tag. T7-tagged ORF1p specifically binds to platelet-derived LINE-1 mRNA indicating that platelets are capable of forming

---

Figure 1 Continued. These images are representative of 4 independent experiments. **F**, Schematic representation of the structural organization of active L1 retroelements. The boundaries of a retroelement are defined by the presence of tandem site duplications (TSDs). L1 elements are composed of a 5′ untranslated region (5′ UTR) that contains an internal RNA polymerase II promoter, followed by 2 ORF1 and ORF2 (open reading frames) and a 3′ UTR containing a polyadenylation signal (pA). Primer binding sites for ORF1 (red) and ORF2 (blue), and the area of in situ probe binding (dark red) are indicated. M indicates marker.
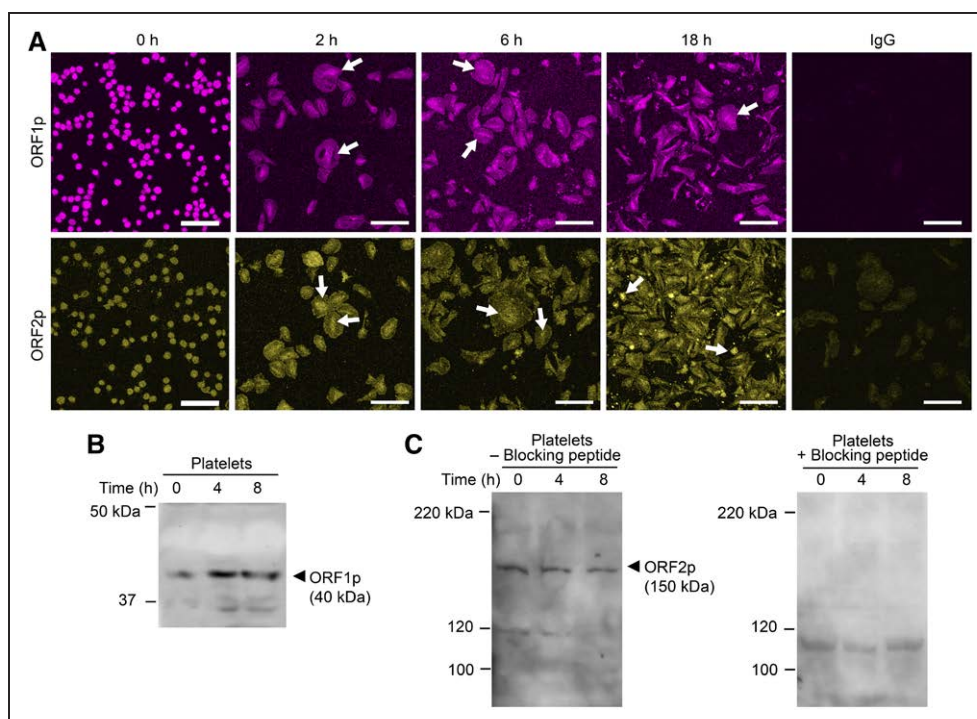
Figure 2. Human platelets express ORF1 (open reading frame) and ORF2 protein. **A**, Freshly isolated platelets were fixed in suspension immediately (baseline, 0 h) or adhered to immobilized fibrinogen in the presence of thrombin for 2, 6, or 18 h. Immunofluorescence staining with an anti-L1 ORF1p (**top** row, magenta stain) and anti-L1 ORF2p (**bottom** row, yellow stain) antibody, respectively, demonstrates expression of both L1-encoded proteins ORF1p and ORF2p in platelets, irrespective of presence or absence of thrombin stimulation. White arrows indicate the time-dependent concentration of L1 proteins in central cell areas, rich in mRNA and ribosomes. The isotype-specific IgG control is shown on the far right (scale bars=10 μm). This figure is representative of 3 independent experiments. **B**, Immunoblot analysis of platelet lysates using the anti-L1 ORF1p antibody. Freshly isolated platelets were immediately fixed in suspension (t=0 h) or allowed to adhere to immobilized fibrinogen in the presence of thrombin for 4 or 8 h. The cells were then lysed and proteins separated by SDS-PAGE electrophoresis. **C**, Immunoblot analysis of platelet lysates using the anti-L1 ORF2p antibody. Platelets were treated as in **B**; however, the samples were split and processed in parallel in the absence (**left**) or presence (**right**) of an ORF2p quenching peptide. Presence of the blocking peptide prevents the detection of L1 ORF2p with the anti-L1 ORF2p antibody. **B**, **C**, Representative of 4 and 5 independent experiments, respectively.

LINE-1 RNPs (Figure 3E). In addition, the experiments confirmed that the RNPs isolated from platelets (Figure 3A) are composed of LINE-1 encoding mRNAs and encoded proteins. After identifying that the major source of eRT activity in platelets is the L1 ORF2p RT domain in isolated RNPs, we next sought to determine the function of eRT activity in platelets.

ERT in Platelets Alters Cytoskeletal Dynamics, Promotes Prothrombotic Functional Responses In Vivo, and Regulates Global Protein Synthesis

Previous studies by our group and others[50,54] demonstrated that cytoskeletal reorganization can promote the formation of extended platelets with ≥2 cell bodies, a process termed progeny formation that resembles how megakaryocytes form new platelets. In tumor cells, inhibition of eRT activity induces cellular differentiation,[37,40] a process that also regulates cytoskeletal events. Therefore, we hypothesized that platelet eRT activity regulates platelet progeny formation; morphological changes in human platelets orchestrated by cytoskeletal dynamics. When platelet eRT activity was inhibited with nevirapine (an RT inhibitor used to treat people with HIV), at doses similar to concentrations seen in treated patients, the number of newly formed cell bodies that extended from cultured platelets significantly increased (Figure 4A).

Platelet cytoskeletal reorganization and progeny formation can result in platelet activation.[50] We next sought to determine whether platelet eRT activity regulated functional responses and thrombosis. We first stimulated platelets pretreated in vitro with nevirapine (or its vehicle control) with thrombin. Inhibition of platelet eRT activity with nevirapine increased activated integrin αIIbβ3 expression on the platelet surface (Figure 4B). To establish whether nevirapine regulated thrombosis in vivo, we first confirmed that similar to human platelets, murine platelets possess eRT activity (Figure IV in the online-only Data Supplement). In a well-established pulmonary thrombosis model,[52] which is platelet dependent, nevirapine significantly accelerated thrombosis-dependent mortality (Figure 4C and 4D). To determine the clinical relevance of these findings, we examined activation of integrin αIIbβ3 in platelets isolated from people with HIV treated with RT inhibitors clinically and matched healthy controls. As shown in Figure 4E, unstimulated platelets from people with HIV had significantly increased basal activation of integrin αIIbβ3, thus recapitulating our in vitro findings (Figure 4B).

On the basis of these in vitro and in vivo results and observations[50] that platelet cytoskeletal events require protein synthesis, we next determined whether eRT activity regulates de novo protein synthesis. We performed metabolic labeling
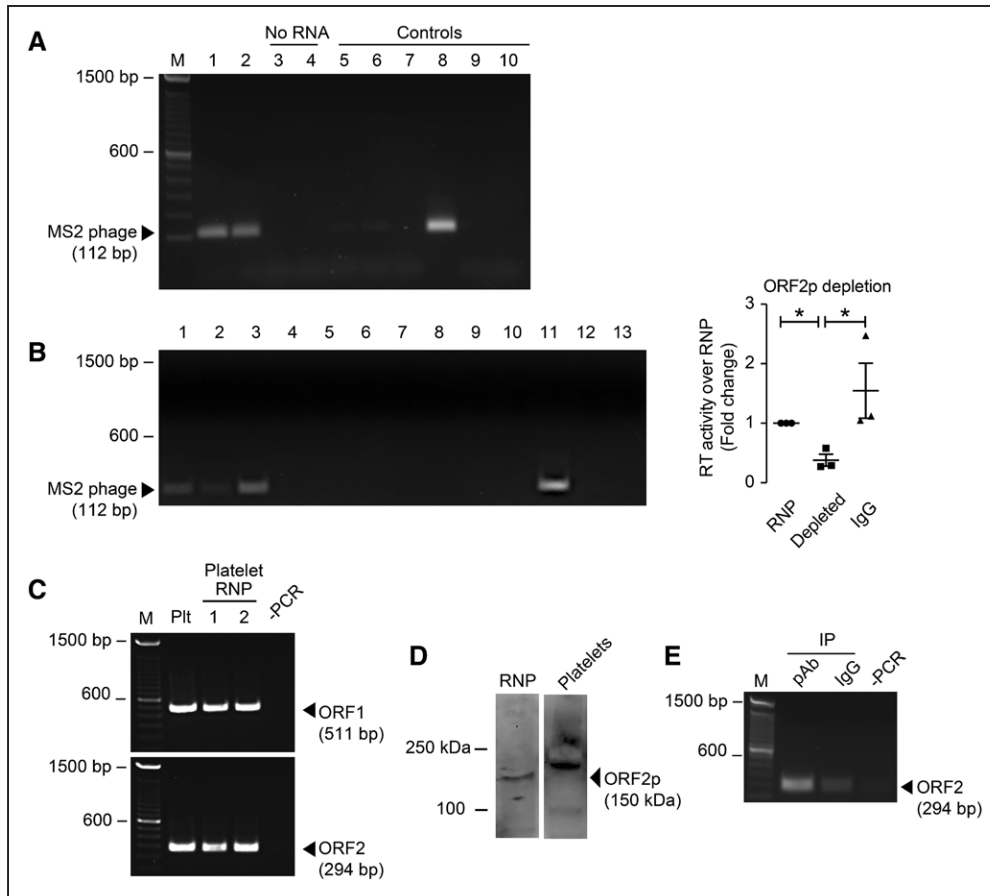
Figure 3. Platelet ribonucleoprotein particles (RNPs) contain L1 RNA and are a source of endogenous reverse transcriptase (eRT) activity. **A**, RT assays with platelet-derived RNPs. RNPs were isolated as described in the Materials and Methods section and incubated with (lanes 1 and 2) or without (lanes 3 and 4) MS2 phage RNA. Controls include: lane 5—platelet lysate replaced with the lysis buffer only; lane 6—omission of the platelet lysate; lane 7—omission of the platelet lysate and MS2 phage RNA; lane 8—platelet lysate replaced with commercial RT; lane 9—omission of the reverse MS2 phage primer; lane 10—negative PCR. This figure is representative of 5 independent experiments. **B**, Depletion of L1 ORF2p (open reading frame) from platelet-derived RNPs. RNPs were isolated as described in the Materials and Methods section, and L1 ORF2p was depleted using immunoprecipitation strategies. Nondepleted (lane 1), depleted (lane 2), or IgG-depleted platelet RNPs (lane 3) were incubated with (lanes 1–3) or without (lanes 4–6) MS2 phage RNA. Controls include lane 7—platelet lysate without MS2 phage RNA; lane 8—RNP replaced with the lysis buffer only; lane 9—omission of the RNP; lane 10—omission of the RNP and MS2 phage RNA; lane 11—platelet lysate replaced with commercial RT; lane 12—omission of the reverse MS2 phage primer; lane 13—negative PCR. The dot blot on the right side represents the densitometric analysis of the nondepleted (RNP), depleted, or IgG-depleted platelet RNPs (IgG), indicating a ≈60% reduction in RT activity (mean±SEM). This figure is representative of 3 independent experiments. *$P<0.05$. **C**, Reverse transcriptase polymerase chain reaction (RT-PCR) on RNA isolated from platelet RNPs. RNA from RNPs was isolated and probed for LINE-1 (long interspersed nuclear element-1) *ORF1* (**top**) and *ORF2* (**bottom**). RNA in 2 different RNP samples [1, 2] was analyzed using PCR and specific primer sets. An unfractionated platelet lysate sample (Plt) was analyzed in parallel. This figure is representative of n=5 independent experiments. **D**, Immunoblot analysis of platelet-derived RNP (**left**), and platelet lysates (**right**) using the anti-L1 ORF2p antibody. This figure is representative of 3 independent experiments. **E**, RT-PCR detecting platelet-derived endogenous L1 RNA/ORF1p interaction. L1 ORF1p was in vitro translated from the expression plasmid pAD2TE1, resulting in a T7-tagged ORF1p. Platelet RNA was isolated and incubated with ORF1p-T7 tag, then immunoprecipitated and analyzed for bound LINE-1 RNA. pAb—IP using anti-T7 antibody, IgG—isotype control, –PCR—control. This figure is representative of 3 independent experiments. IP indicates immunoprecipitation; and M, marker.

by incubating platelets with Click-IT L-azidohomoalanine[50] in the presence or absence of nevirapine. Inhibiting eRT activity significantly increased the incorporation of labeled L-azidohomoalanine into platelets (Figure 4F). The specificity of eRT-regulated translation in platelets was demonstrated by using puromycin (a translational inhibitor) as a control (Figure 4F). These data indicate that eRT activity in platelets regulates protein synthetic events.

To establish the relevance of platelet eRT activity in human disease, we examined the activity and function of eRT in platelets isolated from people with HIV. We confirmed, similar to our observations in platelets from healthy subjects, that platelets from people with HIV (with undetectable viral load) possess eRT activity (data not shown). Next, we incubated platelets isolated from healthy donors or a person with HIV treated with an RT inhibitor with [35S]methionine and [35S]cysteine. Compared with a healthy control subject, protein synthesis was increased in a person with HIV treated clinically with an RT inhibitor (Figure VA in the online-only Data Supplement). Increased protein synthesis was also observed when platelets from a healthy donor were treated with nevirapine ex vivo (Figure VB in the online-only Data Supplement). Furthermore, platelets from people with HIV on ART demonstrated dramatically increased morphological changes (Figure 4G) that require cytoskeletal reorganization.
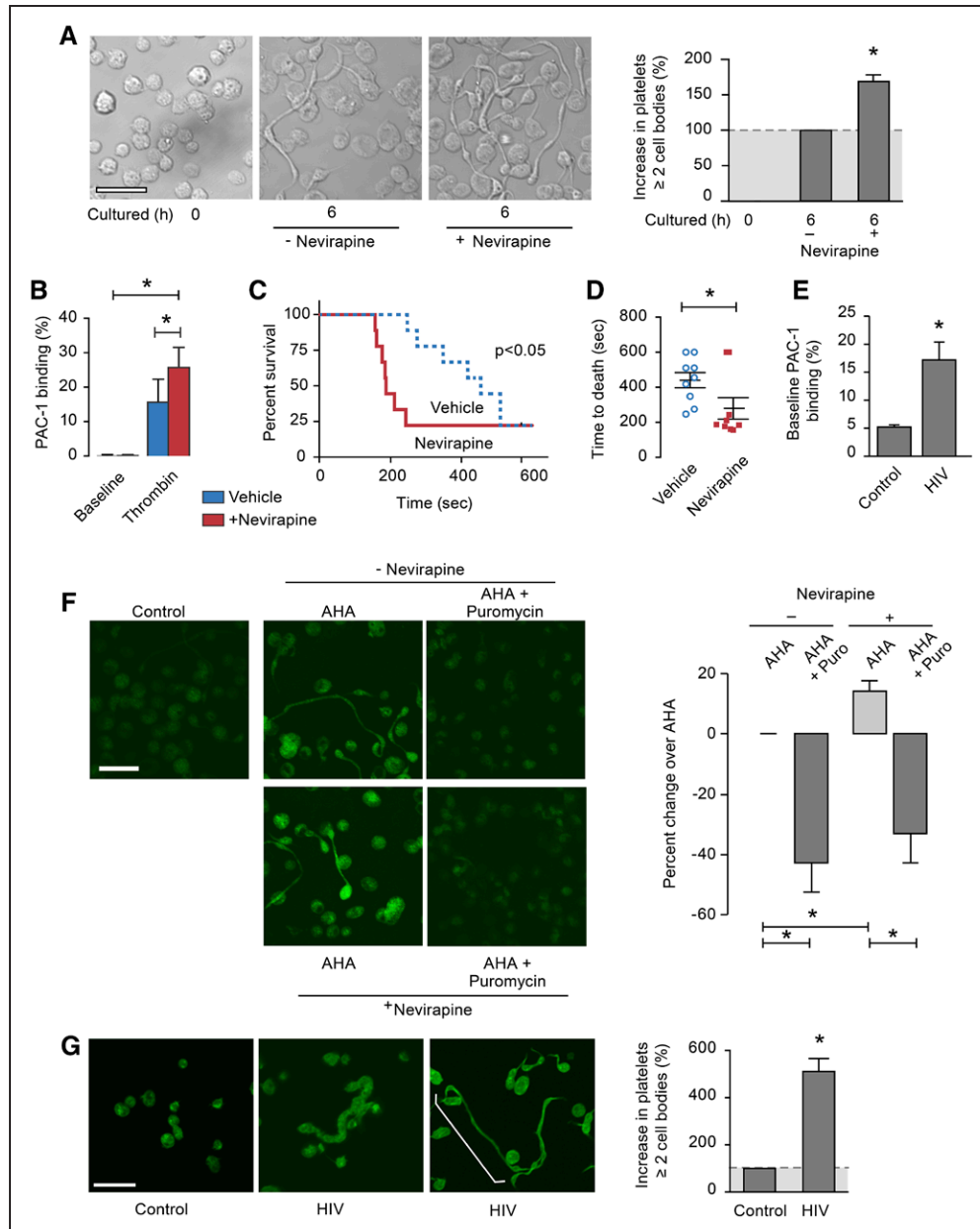
Figure 4. Inhibition of endogenous reverse transcriptase (eRT) activity in platelets alters actin cytoskeletal events, promotes prothrombotic functional responses, and induces global protein synthesis. **A**, Platelets from healthy individuals were isolated and fixed in suspension (0 h), or treated with nevirapine (750 μmol/L) or vehicle (control, DMSO) and subsequently incubated for 6 h. The microscopy images display representative examples of cultured platelets in the absence (–nevirapine) or presence of nevirapine (scale bar=10 μm). The bar graph displays the percent increase in the number of platelets with at least 2 cell bodies in treated vs untreated platelets (mean±SEM; n=8). *P<0.05. **B**, Platelets from healthy individuals were pre-treated with nevirapine for 6 h (750 μmol/L, red) or its vehicle control (DMSO, blue). PAC-1 binding to activated integrin αIIbβ3 on the platelet surface was evaluated by flow cytometry at baseline or after incubation with thrombin (0.1 U/mL for 10 min). The bar graph depicts the mean±SEM. *P<0.05. **C**, Wild-type mice were treated in vivo with either nevirapine (red) or its vehicle (DMSO, blue) by daily gavage for 4 d. Pulmonary embolism was induced by retro-orbital injection of collagen/epinephrine as described in the Materials and Methods. Mortality from respiratory failure was measured to the stopping point of 600 s (10 min). The Kaplan–Meier plot depicts the percent of mice surviving over time. The x axis shows time in still cessation of breathing (n=8–12 mice per group). **D**, Summary blot for the time to death (s) for the individual animals from the experiment shown in (**C**). *P<0.05. **E**, Human platelets from healthy individuals or people with HIV were isolated. PAC-1 binding to activated integrin αIIbβ3 on the platelet surface was evaluated by flow cytometry without additional, exogenous stimulation (ie, baseline). The bar graph depicts the mean±SEM. *P<0.05. **F**, Analysis of de novo protein synthesis in platelets. Freshly isolated platelets were cultured in the presence of an azido-amino acid analog of alanine (L-azidohomoalanine [AHA]), without (**top**) or with (**bottom**) nevirapine. In addition, select samples were pre-incubated with puromycin (AHA+puromycin) or its vehicle (AHA) for 2 h. The platelets were fixed after 6 h, and incorporation of the amino acid analog into protein was visualized (green stain). Unlabeled platelets fixed at baseline (**left**) were used to control for background immunofluorescence (scale bar=10 μm). The bar graph displays the Cell Profiler analysis of the staining intensity for AHA (green) and is expressed as % change over AHA treated cells (±SEM; n=3). *P<0.05. This figure is representative of n=3 independent experiments. **G**, Platelets isolated from healthy individuals (control) and people with HIV were fixed in suspension. The microscopy images display representative examples of platelets isolated from the 2 experimental groups, including representative images from 2 people with HIV (actin stain in green, scale bar=10 μm). The bar graph displays the percent increase in the number of platelets with at least 2 cell bodies (as shown by the white bracket in the far **right**) in people with HIV vs healthy individuals (control; mean±SEM; n=3). *P<0.05.

RNA–DNA Hybrids Are Present in Human Platelets

As our findings suggest that platelet eRT activity controls translational events, we hypothesized that one function of eRT in platelets is to generate RNA–DNA hybrids, resulting in a translational block (Graphic Abstract). We identified RNA–DNA hybrids in human platelets in situ (Figure 5A and 5B). We next determined the mechanisms controlling RNA–DNA hybrid formation. In freshly isolated platelets from healthy control subjects, RNA–DNA hybrids were present in 6.6±3.2% of the cells. When platelets were incubated overnight, the percentage of hybrid-positive cells increased to 20.0±1.6% (Figure 5; *P*<0.05). This increase in hybrid formation was RT dependent because the treatment of platelets

with nevirapine reduced hybrid-positive cells (11.1±2.9%; Figure 5; *P*<0.05). To demonstrate the specificity of the antibody-based hybrid detection, we treated platelets with DNase and RNase A in a low-concentration NaCl buffer, conditions favoring the digestion of DNA or RNA in RNA–DNA hybrids. As expected, both DNase and RNase A significantly reduced hybrid formation (Figure 5). In contrast, using a high concentration of NaCl in combination with RNase A (conditions under which hybrids are not digested) did not decrease hybrid formation.

Yoshida et al[64] also used exogenous MS2 phage RNA to examine RT activity in washed platelet extracts from patients with myeloproliferative neoplasms. They speculated that RT
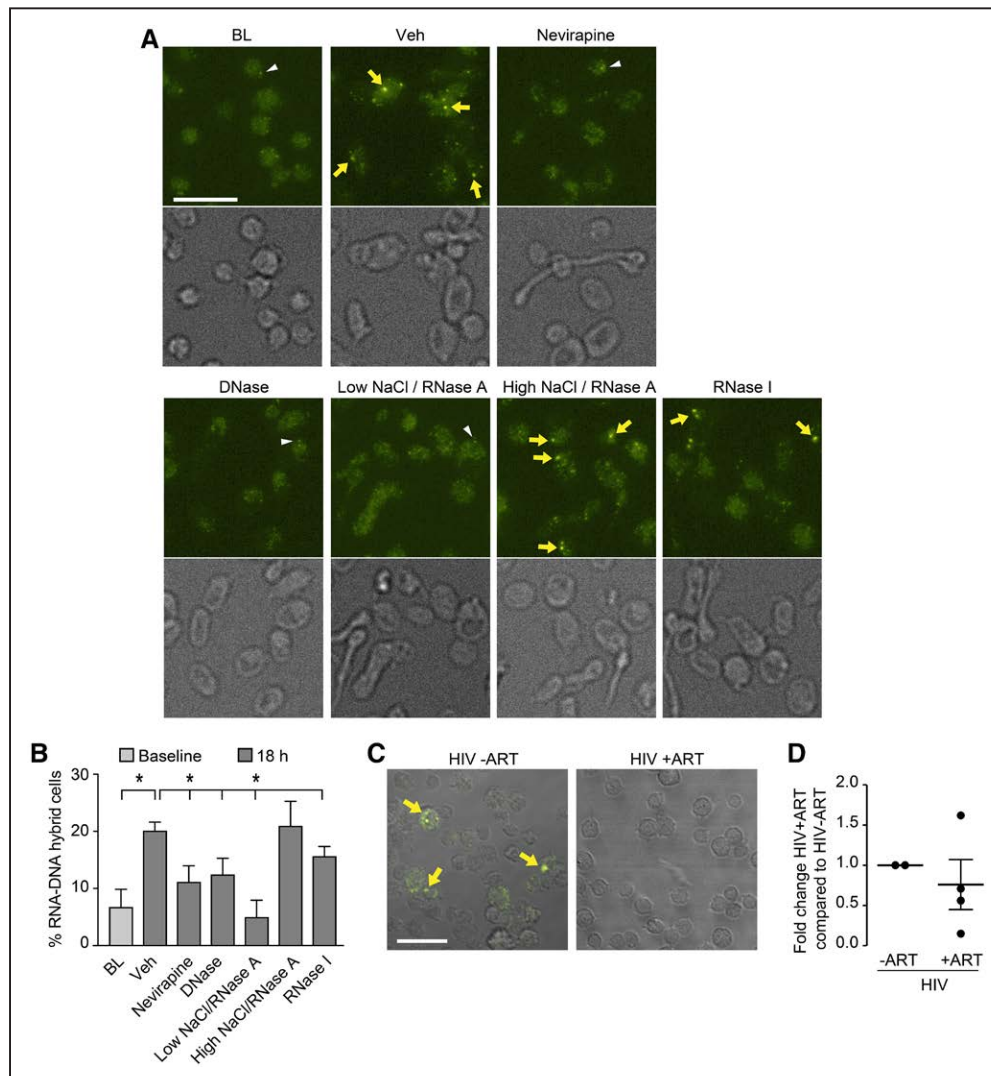
Figure 5. RNA–DNA hybrids are present in human platelets and increased in people with HIV not treated with a reverse transcriptase (RT) inhibitor. **A**, Immunofluorescence analysis of platelets stained with an antihybrid antibody. Platelets were fixed in suspension (BL), or treated with DMSO (Veh) or nevirapine (750 µmol/L) and subsequently incubated for 18 h. RNA–cDNA hybrids were detected using an antihybrid antibody (yellow arrows and white arrowheads). Post-fixation, platelets were treated with Turbo DNase (digests double-strand DNA and DNA in hybrids), RNase A low (NaCl concentration at 70 mmol/L, digests single-strand RNA, double-strand RNA, and RNA in RNA–DNA hybrids), RNase A high (NaCl concentration at 500 mmol/L, digests only single-strand RNA and leave hybrids intact), or RNase I (which digests single- and double-stranded RNA). Scale bar=10 µm. **B**, The bar graph displays the percent of RNA–DNA hybrid-positive cells (mean±SEM; n=3). *P*<0.05, Veh compared with BL, nevirapine treated, low NaCl/RNase A, and RNase I–treated cells. **C**, Confocal images of platelets immunostained with an anti-RNA–DNA hybrid antibody (yellow, arrows). Platelets from people with HIV before the initiation of treatment (HIV −ART) and people with HIV on treatment (HIV +ART) were isolated and fixed in suspension. Scale bar=10 µm. **D**, The bar graph displays the fold change of RNA–DNA hybrid-positive cells in samples from HIV −ART vs HIV +ART (mean±SEM; n=2–4). ART indicates antiretroviral therapy.

activity may be found in mitochondria. While not a primary focus of our studies, in additional control experiments, we stained platelets with mitotracker to detect mitochondria, and the anti-RNA–DNA hybrid antibody in parallel, correlating potential intramitochondrial transcription events resulting in cotranscriptional RNA–DNA hybrid formation. Although some costaining could be detected in platelet mitochondria, ≈50% of the hybrid signals were independent of mitochondrial staining (data not shown). Next, we compared the RNA–DNA hybrid expression levels between platelets isolated from people with HIV before initiation of ART and platelets isolated from people with HIV after treatment with RT inhibitor–based ART. Platelets from people with HIV had reduced numbers of RNA–DNA hybrids, compared with platelets from people with HIV not being treated with RT inhibitor–based ART (Figure 5C and 5D).

To identify candidates regulated by RNA–DNA hybrids, we immunoprecipitated hybrids from platelet lysates from healthy control subjects. RNA–DNA hybrids were isolated, a cDNA library of these RNAs was created, and sequencing was performed. Sequence analysis of the cDNA library revealed the enrichment of several target RNAs (Table I in the online-only Data Supplement). Three of the enriched identified RNAs coded for *MAP1LC3B* (microtubule-associated protein 1 light chain 3 β), *SELP* (P-selectin, which regulates platelet activation), and *RPL26* (ribosomal protein L26, which

regulates gene expression; Figure 6A). MAP1LC3B mediates autophagy,[65,66] and autophagy has been linked to platelet activation.[67] Accordingly, we focused on validating the presence of *MAP1LC3B* nucleotide sequences. Enrichment of *MAP1LC3B* sequences within RNA–DNA hybrids was confirmed in subsequent IP and qPCR experiments (Figure 6B). Thus, *MAP1LC3B* mRNA is expressed within RNA–DNA hybrids in platelets.

LINE-1 ORF1p Interacts With *MAP1LC3B* RNA in Trans

To determine if *MAP1LC3B* mRNA can be a substrate for LINE-1 ORF1p and ORF2p, we in vitro translated T7-tagged ORF1p from the expression plasmid pAD2TE1[27] as a template (Figure 3E). Platelet RNA was incubated with the recombinant T7-tagged ORF1p and immunoprecipitated using an anti-T7 tag antibody. ORF1p binds to platelet-derived *MAP1LC3B* mRNA (Figure 6C) indicating that this mRNA is associated with LINE-1 RNPs and would, therefore, be accessible to the RT domain of LINE-1 ORF2p.

RNA–DNA Hybrids Regulate Protein Synthetic Events in Human Platelets

We next in vitro transcribed an MAP1LC3B-myc-DDK-tag encoding plasmid, generating an mRNA template for a modified in vitro RT activity assay and allowing us to specifically
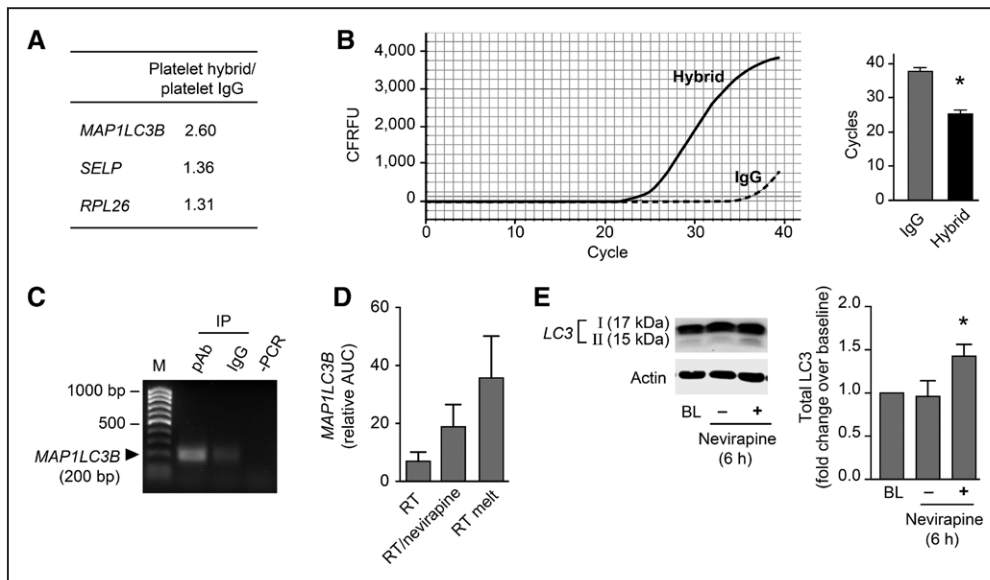
Figure 6. RNA–DNA hybrids serve as translational repressors in human platelets. **A**, Fold enrichment of coimmunoprecipitated RNA–DNA hybrids that were sequenced with targets identified (mRNAs coding for microtubule-associated protein 1 light chain 3 β (*MAP1LC3B*), *SELP*—P-selectin, and *RPL26*—ribosomal protein L26) when comparing IgG vs specific antihybrid antibody. **B**, *MAP1LC3B* was verified using qPCR. An example of the real-time tracing is depicted on the **left** (CFRFU [curve fit relative fluorescence units]). The bar graph shows the change in cycle number threshold (mean±SEM; n=3, *P<0.05). **C**, Reverse transcriptase polymerase chain reaction analysis to demonstrate the presence of *MAP1LC3B* RNA in L1 ORF1p-T7 immunoprecipitates. T7-tagged L1 ORF1p was in vitro translated from the pAD2TE1 expression plasmid. Platelet RNA was isolated and incubated with ORF1p-T7 tag, immunoprecipitated, and analyzed for bound *MAP1LC3B* RNA. pAb—IP using anti-T7 antibody, IgG—isotype control, –PCR—control for contaminants. This figure is representative of 3 independent experiments. **D**, MAP1LC3B was in vitro transcribed, and the mRNA reverse transcribed using a reverse transcriptase (RT) activity assay, however, with shortened extension time (15 min, RT). Select samples were pre-incubated with nevirapine (500 µmol/L, 45 min, 37°C, RT+nevirapine), or processed using a 2-min melting step (95°C, RT melt). The mRNA or RNA–DNA hybrids were subsequently introduced into an in vitro translation assay, and resulting MAP1LC3B protein was separated by SDS-PAGE and detected using an anti-myc-DDK tag antibody. The bar graph of the densitometric analysis is shown. **E**, Platelets were lysed at baseline (0 h), or treated with DMSO control or nevirapine (750 µmol/L) and subsequently incubated for 6 h. Total MAP1LC3B (LC3B) was detected by means of Western blotting. LC3 isoforms I and II were detected and analyzed using ImageJ. A representative Western Blot for LC3 and the corresponding control actin blot are depicted (**left**). The bar graph (**right**) displays the fold change of total LC3 of the 6 h samples over baseline. *P<0.05. This figure is representative of n=4 independent experiments. IP indicates immunoprecipitation.

detect the translated MAP1LC3B fusion protein. Some platelet lysates used in the RT activity assay as RT donor were treated with the RT inhibitor nevirapine to block hybrid formation. In addition, select samples underwent a melting step, resulting in a separation of RNA–DNA hybrids and releasing the translational block. The cDNA/hybrids were in vitro translated, and the resulting proteins were separated by SDS-PAGE using a myc-DDK tag antibody for detection of in vitro translated proteins. The bar graph (Figure 6D) demonstrates that inhibiting hybrid formation (either by nevirapine or by inducing melting of the RNA from the DNA) increased the synthesis of MAP1LC3B protein. As these data suggest that MAP1LC3B synthesis in platelets may be translationally controlled, at least in part, by RNA–DNA hybrids, we next examined MAP1LC3B expression in live platelets pre-treated with nevirapine. Nevirapine significantly increased total MAP1LC3B protein (LC3B I and LC3B II) in platelets (Figure 6E). Similar findings were observed with 2 other proteins: P-selectin and ribosomal protein L26 (Figure VIA and VIB in the online-only Data Supplement). P-selectin surface translocation to the platelet surface was also increased in people with HIV treated with RT inhibitors (Figure VIC in the online-only Data Supplement). These data indicate that nevirapine inhibits RNA–DNA hybrid formation and enhances protein synthesis by releasing a translational block.

Discussion

Platelets are anucleate and traditionally viewed as having a fixed molecular signature and associated functional responses. Nevertheless, platelets use an ever-increasing, and often unexpected, repertoire of mechanisms to regulate their transcriptional and proteomic signature in health and disease.[2] Here, we provide the first evidence that human platelets possess LINE-1–derived eRT activity, regulating platelet morphology and protein synthesis, and leading to prothrombotic functional responses in vitro and in vivo. We also demonstrate that these findings are concordantly observed in people with HIV clinically treated with RT inhibitors.

Both LINE-1 ORF1p (RNA binding) and ORF2p (endonuclease and RT domain) are encoded by the bicistronic LINE-1 and expressed in platelets. Concordant with the detected expression of both LINE-1 proteins, we discovered that platelets possess eRT activity (Figure 1). Previous studies have demonstrated the importance of LINE-1 RNPs,[27,30,53] intracellular complexes that are integral to the regulation of gene expression[63] and for retrotransposition in other cell types. Consistent with this, we report that the majority of platelet eRT activity is localized to LINE-1 RNPs (Figure 3). Depleting LINE-1 ORF2p from platelet RNPs demonstrates that LINE-1 RNPs are the major (eg, ≈60% of greater) contributor to platelet eRT activity. Furthermore, we show that exogenously expressed LINE-1 ORF1p containing an epitope tag (T7) at the carboxy terminus binds selectively to its endogenous encoding RNA (cis-preference[30]) in platelets. These findings indicate that human platelets contain functional LINE-1 RNPs. When platelets were incubated on immobilized fibrinogen and stimulated with thrombin, we observed trafficking of the LINE-1 proteins toward the central areas of platelets (Figure 2), subcellular regions known to be rich in

mRNAs and ribosomal constituents.[7,8] This shift in localization would allow LINE-1 proteins to interact with endogenous mRNAs that code for other cellular proteins (transacting LINE-1), a concept evaluated in previous studies.[30]

Because LINE-1 ORF2p includes an RT domain, it is worth discussing the functions of RT enzymes. In biochemical in vitro assays, RTs are used to reverse transcribe mRNA into cDNA to enable the subsequent PCR amplification step. This reaction forms mRNA–cDNA hybrids. Here, we demonstrate that platelets dynamically express RNA–DNA hybrids. Hybrid expression was dependent on eRT (ORF2p), and hybrid formation was blocked by nevirapine at doses achieving concentrations relevant to patients treated with this drug.

On the basis of our findings, we propose a previously unrecognized cellular mechanism. In our model, eRT in platelets generates RNA–DNA hybrids that block translation by partially reverse transcribing mRNA (Graphic Abstract). The cellular concept of intentionally stalling translation was used in molecular biology strategies as an in vitro technique to identify specifically translated mRNAs,[42,43] but to date has not been identified as an actively used translational control mechanism in primary human cells. In contrast, it is a well-accepted concept that the stability of cotranscriptional RNA–DNA hybrids affects transcriptional efficiency[44] and even that stability differs between coding and noncoding regions.[68] However, this transcriptional mechanism is not based on eRT utilization. Nevertheless, in 2013, Sciamanna et al[70] suggested that the regulation of tumor cell biology by LINE-1,[36,37,39,70] an area of intense research, could be induced by the formation of RNA–DNA hybrids. Using CsCl density gradients, they selectively identified *Alu* and LINE-1 containing RNA–DNA hybrid molecules in cancer but not in normal cells. They concluded that LINE-1–mediated RNA–DNA hybrids would interfere with the formation of dsRNA and, therefore, the synthesis of regulatory small RNAs.[69]

Our findings demonstrate that RNA–DNA hybrid formation regulates synthesis of specific candidate RNAs by the induction of a translational block. This is supported directly by protein de novo synthesis assays, but also indirectly by the formation of platelet progeny, a process strictly dependent on protein synthetic activity.[50] *MAP1LC3B* was identified as one of the target mRNAs of transacting L1 ORF1p. MAP1LC3B plays an important role in autophagic processes[65,66] and serves as a good autophagy marker.[71] In addition, this catabolic process maintaining cellular hemostasis, adaptation to starvation, development, and pathogen elimination needs to be tightly regulated.[72] Therefore, the translational control of one of the major players in autophagy by RNA–DNA hybrid formation is an attractive focus of future research. Two other identified hybrids also underscore the importance of this novel regulatory pathway. RPL26 is important for ribosomal hemostasis and regulation of gene expression, whereas SELP (P-selectin) is one of the major α-granular constituents being translocated to the surface of activated platelets on stimulation.[73]

This novel mechanism for translational control has clinical implications. As part of ART, patients with HIV are typically prescribed RT inhibitor–based therapy. In people with HIV, the introduction of ART has dramatically improved life expectancy.[46] As a result, chronic and often accelerated disorders,

including atherothrombosis,[47–49] are replacing opportunistic infections as important causes of morbidity and mortality.[74] Furthermore, in patients with HIV under ART, and despite undetectable virus levels, a 30-fold increase in mortality when compared with uninfected controls could be demonstrated. The increased mortality was attributed to ongoing innate immune responses and activation of coagulation factors.[75–77]

We demonstrated that platelet eRT activity regulates integration activation in vitro and in vivo. Similar findings of platelet integrin activation were observed in people with HIV prescribed ARTs that include RT inhibitors. We postulate that inhibition of platelet eRT activity may contribute to the increased risk of thrombosis observed in people with HIV.[78] Furthermore, because we detected LINE-1 expression in other primary human blood cells, including megakaryocytes and T cells (Figure VIII in the online-only Data Supplement), our findings may have implications not only in the megakaryocyte–platelet axis but also in other cell lineages.

Platelets isolated from people with HIV were more synthetically active (Figure V in the online-only Data Supplement) and had altered morphology resembling dumbbells (Figure 4C, as seen in vitro with nevirapine treated platelets), suggesting deregulated translational control mechanisms. Consistent with these observations, hybrids were higher in platelets from patients with HIV not treated with ART than compared with healthy individuals or people with HIV treated with ART. Our findings suggest that administration of ART to people with HIV alters platelet protein synthesis by lifting the RNA–DNA hybrid-induced translational block, although we cannot exclude the possibility that differences in RNA–DNA hybrids in people with HIV was also induced by HIV encoded RT. In this context, it is also interesting to note that platelets contain dengue virus DNA when infected with dengue virus, a (+)ssRNA virus (Figure VII in the online-only Data Supplement). Dengue virus DNA is not part of the virus life cycle, and these data suggest a reverse transcription event. Furthermore, when eRT was inhibited, dengue DNA could not be detected. One might speculate if inhibiting dengue DNA formation removes an RNA–DNA hybrid-induced translational block, leading to increased dengue virus replication.

Although our findings confirm and extend prior studies in murine cells and tumor lines,[37,39,79] we recognize that several reports did not confirm that nevirapine blocks LINE-1 RT.[80] There are several potential explanations for these seemingly contradictory findings. First, we used higher concentrations of nevirapine (750 µmol/L), specifically chosen to recapitulate systemic concentrations of nevirapine achieved clinically. Second, we did not use tumor cell lines, but primary human cells (eg, platelets). Finally, we examined RNA–DNA hybrid formation, rather than retrotransposition events. We also identified that another RT inhibitor, delavirdine, similarly blocked eRT activity (data not shown), indicating that our findings are not confined to nevirapine alone. Although size exclusion experiments (Figure I in the online-only Data Supplement) did not completely exclude the possibility of eRT activity deriving from proviral insertions of human endogenous retroviruses, the fully processed HERV-K RT has a molecular weight of 66 kDa, making this unlikely.

In conclusion, our data identify a previously unrecognized function for LINE-1–encoded proteins. We propose a model whereby endogenous LINE-1–mediated RNA–DNA hybrid formation controls protein expression for select mRNAs (Graphic Abstract). Because LINE-1 is classically considered to be involved in disease inducing de novo disruption of gene expression by retrotransposition events,[35] or tumor genesis,[81,82] our findings also demonstrate that in human platelets, LINE-1 functions in a newly described constructive and potentially regulated fashion. Finally, our results provide evidence for a new translational regulatory mechanism that is present in platelets and which regulates integrin activation and thrombosis.

Disclosures
None.

References

1. Schwertz H, Rowley JW, Tolley ND, Campbell RA, Weyrich AS. Assessing protein synthesis by platelets. *Methods Mol Biol*. 2012;788:141–153. doi: 10.1007/978-1-61779-307-3_11.
2. Weyrich AS, Schwertz H, Kraiss LW, Zimmerman GA. Protein synthesis by platelets: historical and new perspectives. *J Thromb Haemost*. 2009;7:241–246. doi: 10.1111/j.1538-7836.2008.03211.x.
3. Weyrich AS, Dixon DA, Pabla R, Elstad MR, McIntyre TM, Prescott SM, Zimmerman GA. Signal-dependent translation of a regulatory protein, Bcl-3, in activated human platelets. *Proc Natl Acad Sci USA*. 1998;95:5556–5561.
4. Zimmerman GA, Weyrich AS. Signal-dependent protein synthesis by activated platelets: new pathways to altered phenotype and function. *Arterioscler Thromb Vasc Biol*. 2008;28:s17–s24. doi: 10.1161/ATVBAHA.107.160218.
5. Tang H, Hornstein E, Stolovich M, Levy G, Livingstone M, Templeton D, Avruch J, Meyuhas O. Amino acid-induced translation of TOP mRNAs is fully dependent on phosphatidylinositol 3-kinase-mediated signaling, is partially inhibited by rapamycin, and is independent of S6K1 and rpS6 phosphorylation. *Mol Cell Biol*. 2001;21:8671–8683. doi: 10.1128/MCB.21.24.8671-8683.2001.
6. Hsieh AC, Liu Y, Edlind MP, et al. The translational landscape of mTOR signalling steers cancer initiation and metastasis. *Nature*. 2012;485:55–61. doi: 10.1038/nature10912.

7. Denis MM, Tolley ND, Bunting M, et al. Escaping the nuclear confines: signal-dependent pre-mRNA splicing in anucleate platelets. *Cell*. 2005;122:379–391. doi: 10.1016/j.cell.2005.06.015.

8. Schwertz H, Tolley ND, Foulks JM, Denis MM, Risenmay BW, Buerke M, Tilley RE, Rondina MT, Harris EM, Kraiss LW, Mackman N, Zimmerman GA, Weyrich AS. Signal-dependent splicing of tissue factor pre-mRNA modulates the thrombogenicity of human platelets. *J Exp Med*. 2006;203:2433–2440. doi: 10.1084/jem.20061302.

9. Shashkin PN, Brown GT, Ghosh A, Marathe GK, McIntyre TM. Lipopolysaccharide is a direct agonist for platelet RNA splicing. *J Immunol*. 2008;181:3495–3502.

10. Beck CR, Garcia-Perez JL, Badge RM, Moran JV. LINE-1 elements in structural variation and disease. *Annu Rev Genomics Hum Genet*. 2011;12:187–215. doi: 10.1146/annurev-genom-082509-141802.

11. Ostertag EM, Kazazian HH Jr. Biology of mammalian L1 retrotransposons. *Annu Rev Genet*. 2001;35:501–538. doi: 10.1146/annurev. genet.35.102401.091032.

12. Lander ES, Linton LM, Birren B, et al; International Human Genome Sequencing Consortium. Initial sequencing and analysis of the human genome. *Nature*. 2001;409:860–921. doi: 10.1038/35057062.

13. Penzkofer T, Jäger M, Figlerowicz M, Badge R, Mundlos S, Robinson PN, Zemojtel T. L1Base 2: more retrotransposition-active LINE-1s, more mammalian genomes. *Nucleic Acids Res*. 2017;45(D1):D68–D73. doi: 10.1093/nar/gkw925.

14. Loeb DD, Padgett RW, Hardies SC, Shehee WR, Comer MB, Edgell MH, Hutchison CA III. The sequence of a large L1Md element reveals a tandemly repeated 5' end and several features found in retrotransposons. *Mol Cell Biol*. 1986;6:168–182.

15. Scott AF, Schmeckpeper BJ, Abdelrazik M, Comey CT, O'Hara B, Rossiter JP, Cooley T, Heath P, Smith KD, Margolet L. Origin of the human L1 elements: proposed progenitor genes deduced from a consensus DNA sequence. *Genomics*. 1987;1:113–125.

16. McMillan JP, Singer MF. Translation of the human LINE-1 element, L1Hs. *Proc Natl Acad Sci USA*. 1993;90:11533–11537.

17. Alisch RS, Garcia-Perez JL, Muotri AR, Gage FH, Moran JV. Unconventional translation of mammalian LINE-1 retrotransposons. *Genes Dev*. 2006;20:210–224. doi: 10.1101/gad.1380406.

18. Hohjoh H, Singer MF. Sequence-specific single-strand RNA binding protein encoded by the human LINE-1 retrotransposon. *EMBO J*. 1997;16:6034–6043. doi: 10.1093/emboj/16.19.6034.

19. Kolosha VO, Martin SL. In vitro properties of the first ORF protein from mouse LINE-1 support its role in ribonucleoprotein particle formation during retrotransposition. *Proc Natl Acad Sci USA*. 1997;94:10155–10160.

20. Martin SL, Li J, Weisz JA. Deletion analysis defines distinct functional domains for protein-protein and nucleic acid interactions in the ORF1 protein of mouse LINE-1. *J Mol Biol*. 2000;304:11–20. doi: 10.1006/jmbi.2000.4182.

21. Fanning T, Singer M. The LINE-1 DNA sequences in four mammalian orders predict proteins that conserve homologies to retrovirus proteins. *Nucleic Acids Res*. 1987;15:2251–2260.

22. Feng Q, Moran JV, Kazazian HH Jr, Boeke JD. Human L1 retrotransposon encodes a conserved endonuclease required for retrotransposition. *Cell*. 1996;87:905–916.

23. Mathias SL, Scott AF, Kazazian HH Jr, Boeke JD, Gabriel A. Reverse transcriptase encoded by a human transposable element. *Science*. 1991;254:1808–1810.

24. Esnault C, Maestre J, Heidmann T. Human LINE retrotransposons generate processed pseudogenes. *Nat Genet*. 2000;24:363–367. doi: 10.1038/74184.

25. Wei W, Gilbert N, Ooi SL, Lawler JF, Ostertag EM, Kazazian HH, Boeke JD, Moran JV. Human L1 retrotransposition: cis preference versus trans complementation. *Mol Cell Biol*. 2001;21:1429–1439. doi: 10.1128/MCB.21.4.1429-1439.2001.

26. Hohjoh H, Singer MF. Cytoplasmic ribonucleoprotein complexes containing human LINE-1 protein and RNA. *EMBO J*. 1996;15:630–639.

27. Kulpa DA, Moran JV. Ribonucleoprotein particle formation is necessary but not sufficient for LINE-1 retrotransposition. *Hum Mol Genet*. 2005;14:3237–3248. doi: 10.1093/hmg/ddi354.

28. Dewannieux M, Esnault C, Heidmann T. LINE-mediated retrotransposition of marked Alu sequences. *Nat Genet*. 2003;35:41–48. doi: 10.1038/ng1223.

29. Raiz J, Damert A, Chira S, Held U, Klawitter S, Hamdorf M, Löwer J, Strätling WH, Löwer R, Schumann GG. The non-autonomous retrotransposon SVA is trans-mobilized by the human LINE-1 protein machinery. *Nucleic Acids Res*. 2012;40:1666–1683. doi: 10.1093/nar/gkr863.

30. Kulpa DA, Moran JV. Cis-preferential LINE-1 reverse transcriptase activity in ribonucleoprotein particles. *Nat Struct Mol Biol*. 2006;13:655–660. doi: 10.1038/nsmb1107.

31. Elbarbary RA, Lucas BA, Maquat LE. Retrotransposons as regulators of gene expression. *Science*. 2016;351:aac7247. doi: 10.1126/science.aac7247.

32. Chen JM, Férec C, Cooper DN. LINE-1 endonuclease-dependent retrotranspositional events causing human genetic disease: mutation detection bias and multiple mechanisms of target gene disruption. *J Biomed Biotechnol*. 2006;2006:56182. doi: 10.1155/JBB/2006/56182.

33. Mätlik K, Redik K, Speek M. L1 antisense promoter drives tissue-specific transcription of human genes. *J Biomed Biotechnol*. 2006;2006:71753. doi: 10.1155/JBB/2006/71753.

34. Han JS, Szak ST, Boeke JD. Transcriptional disruption by the L1 retrotransposon and implications for mammalian transcriptomes. *Nature*. 2004;429:268–274. doi: 10.1038/nature02536.

35. Hancks DC, Kazazian HH Jr. Roles for retrotransposon insertions in human disease. *Mob DNA*. 2016;7:9. doi: 10.1186/s13100-016-0065-9.

36. Landriscina M, Fabiano A, Altamura S, Bagalà C, Piscazzi A, Cassano A, Spadafora C, Giorgino F, Barone C, Cignarelli M. Reverse transcriptase inhibitors down-regulate cell proliferation in vitro and in vivo and restore thyrotropin signaling and iodine uptake in human thyroid anaplastic carcinoma. *J Clin Endocrinol Metab*. 2005;90:5663–5671. doi: 10.1210/jc.2005-0367.

37. Mangiacasale R, Pittoggi C, Sciamanna I, Careddu A, Mattei E, Lorenzini R, Travaglini L, Landriscina M, Barone C, Nervi C, Lavia P, Spadafora C. Exposure of normal and transformed cells to nevirapine, a reverse transcriptase inhibitor, reduces cell growth and promotes differentiation. *Oncogene*. 2003;22:2750–2761. doi: 10.1038/sj.onc.1206354.

38. Sciamanna I, Barberi L, Martire A, Pittoggi C, Beraldi R, Giordano R, Magnano AR, Hogdson C, Spadafora C. Sperm endogenous reverse transcriptase as mediator of new genetic information. *Biochem Biophys Res Commun*. 2003;312:1039–1046.

39. Sciamanna I, Landriscina M, Pittoggi C, Quirino M, Mearelli C, Beraldi R, Mattei E, Serafino A, Cassano A, Sinibaldi-Vallebona P, Garaci E, Barone C, Spadafora C. Inhibition of endogenous reverse transcriptase antagonizes human tumor growth. *Oncogene*. 2005;24:3923–3931. doi: 10.1038/sj.onc.1208562.

40. Sinibaldi-Vallebona P, Lavia P, Garaci E, Spadafora C. A role for endogenous reverse transcriptase in tumorigenesis and as a target in differentiating cancer therapy. *Genes Chromosomes Cancer*. 2006;45:1–10. doi: 10.1002/gcc.20266.

41. Spadafora C. Endogenous reverse transcriptase: a mediator of cell proliferation and differentiation. *Cytogenet Genome Res*. 2004;105:346–350. doi: 10.1159/000078207.

42. Cooper JA, Moss B. Translation of specific vaccinia virus RNAs purified as RNA-DNA hybrids on potassium iodide gradients. *Nucleic Acids Res*. 1979;6:3599–3612.

43. Dudley K. Hybrid-arrested translation. *Methods Mol Biol*. 1988;4:39–45. doi: 10.1385/0-89603-127-6:39.

44. Nudler E, Mustaev A, Lukhtanov E, Goldfarb A. The RNA-DNA hybrid maintains the register of transcription by preventing backtracking of RNA polymerase. *Cell*. 1997;89:33–41.

45. Ohle C, Tesorero R, Schermann G, Dobrev N, Sinning I, Fischer T. Transient RNA-DNA hybrids are required for efficient double-strand break repair. *Cell*. 2016;167:1001.e7–1013.e7. doi: 10.1016/j.cell.2016.10.001.

46. Mellors JW, Rinaldo CR Jr, Gupta P, White RM, Todd JA, Kingsley LA. Prognosis in HIV-1 infection predicted by the quantity of virus in plasma. *Science*. 1996;272:1167–1170.

47. Massberg S, Brand K, Grüner S, Page S, Müller E, Müller I, Bergmeier W, Richter T, Lorenz M, Konrad I, Nieswandt B, Gawaz M. A critical role of platelet adhesion in the initiation of atherosclerotic lesion formation. *J Exp Med*. 2002;196:887–896.

48. Mastenbroek TG, van Geffen JP, Heemskerk JW, Cosemans JM. Acute and persistent platelet and coagulant activities in atherothrombosis. *J Thromb Haemost*. 2015;13(suppl 1):S272–S280. doi: 10.1111/jth.12972.

49. Weyrich A, Cipollone F, Mezzetti A, Zimmerman G. Platelets in atherothrombosis: new and evolving roles. *Curr Pharm Des*. 2007;13:1685–1691.

50. Schwertz H, Köster S, Kahr WH, Michetti N, Kraemer BF, Weitz DA, Blaylock RC, Kraiss LW, Greinacher A, Zimmerman GA, Weyrich AS. Anucleate platelets generate progeny. *Blood*. 2010;115:3801–3809. doi: 10.1182/blood-2009-08-239558.

51. Rondina MT, Freitag M, Pluthero FG, Kahr WH, Rowley JW, Kraiss LW, Franks Z, Zimmerman GA, Weyrich AS, Schwertz H. Non-genomic

activities of retinoic acid receptor alpha control actin cytoskeletal events in human platelets. *J Thromb Haemost*. 2016;14:1082–1094.

52. Rowley JW, Chappaz S, Corduan A, Chong MM, Campbell R, Khoury A, Manne BK, Wurtzel JG, Michael JV, Goldfinger LE, Mumaw MM, Nieman MT, Kile BT, Provost P, Weyrich AS. Dicer1-mediated miRNA processing shapes the mRNA profile and function of murine platelets. *Blood*. 2016;127:1743–1751. doi: 10.1182/blood-2015-07-661371.

53. Doucet AJ, Hulme AE, Sahinovic E, Kulpa DA, Moldovan JB, Kopera HC, Athanikar JN, Hasnaoui M, Bucheton A, Moran JV, Gilbert N. Characterization of LINE-1 ribonucleoprotein particles. *PLoS Genet*. 2010;6:e1001150.

54. Thon JN, Montalvo A, Patel-Hett S, Devine MT, Richardson JL, Ehrlicher A, Larson MK, Hoffmeister K, Hartwig JH, Italiano JE Jr. Cytoskeletal mechanics of proplatelet maturation and platelet release. *J Cell Biol*. 2010;191:861–874. doi: 10.1083/jcb.201006102.

55. Neuhoff V, Arold N, Taube D, Ehrhardt W. Improved staining of proteins in polyacrylamide gels including isoelectric focusing gels with clear background at nanogram sensitivity using coomassie brilliant blue g-250 and r-250. *Electrophoresis*. 1988;9:255–262.

56. Schwertz H, Carter JM, Abdudureheman M, Russ M, Buerke U, Schlitt A, Muller-Werdan U, Prondzinsky R, Werdan K, Buerke M. Myocardial ischemia/reperfusion causes vdac phosphorylation which is reduced by cardioprotection with a p38 map kinase inhibitor. *Proteomics*. 2007;7:4579–4588.

57. Rowley JW, Oler AJ, Tolley ND, Hunter BN, Low EN, Nix DA, Yost CC, Zimmerman GA, Weyrich AS. Genome-wide rna-seq analysis of human and mouse platelet transcriptomes. *Blood*. 2011;118:e101–e111.

58. Kahr WH, Hinckley J, Li L, et al. Mutations in nbeal2, encoding a beach protein, cause gray platelet syndrome. *Nat Genet*. 2011;43:738–740.

59. Hottz ED, Oliveira MF, Nunes PC, Nogueira RM, Valls-de-Souza R, Da Poian AT, Weyrich AS, Zimmerman GA, Bozza PT, Bozza FA. Dengue induces platelet activation, mitochondrial dysfunction and cell death through mechanisms that involve dc-sign and caspases. *J Thromb Haemost*. 2013;11:951–962.

60. Carpenter AE, Jones TR, Lamprecht MR, Clarke C, Kang IH, Friman O, Guertin DA, Chang JH, Lindquist RA, Moffat J, Golland P, Sabatini DM. Cellprofiler: Image analysis software for identifying and quantifying cell phenotypes. *Genome Biol*. 2006;7:R100.

61. Jones TR, Kang IH, Wheeler DB, Lindquist RA, Papallo A, Sabatini DM, Golland P, Carpenter AE. Cellprofiler analyst: data exploration and analysis software for complex image-based screens. *BMC Bioinformatics*. 2008;9:482.

62. Kothapalli R, Danyluck GM, Bailey RD, Loughran TP Jr. Problems associated with product enhancement reverse transcriptase assay using bacteriophage MS2 RNA as a template. *J Virol Methods*. 2003;109:203–207.

63. Mansfield KD, Keene JD. The ribonome: a dominant force in co-ordinating gene expression. *Biol Cell*. 2009;101:169–181. doi: 10.1042/BC20080055.

64. Yoshida S, Yamada H, Sakurai T, Suzuki M, Kojima K. Re-examination by improved reverse transcriptase assay of DNA polymerase in platelets from myelodysplastic disease patients. *Biochem Int*. 1989;19:1133–1141.

65. Feng W, Chang C, Luo D, Su H, Yu S, Hua W, Chen Z, Hu H, Liu W. Dissection of autophagy in human platelets. *Autophagy*. 2014;10:642–651. doi: 10.4161/auto.27832.

66. Klionsky DJ, Abdelmohsen K, Abe A, et al. Guidelines for the use and interpretation of assays for monitoring autophagy (3rd edition). *Autophagy*. 2016;12:1–222.

67. Ouseph MM, Huang Y, Banerjee M, et al. Autophagy is induced upon platelet activation and is essential for hemostasis and thrombosis. *Blood*. 2015;126:1224–1233. doi: 10.1182/blood-2014-09-598722.

68. Kraeva RI, Krastev DB, Roguev A, Ivanova A, Nedelcheva-Veleva MN, Stoynov SS. Stability of mRNA/DNA and DNA/DNA duplexes affects mRNA transcription. *PLoS One*. 2007;2:e290. doi: 10.1371/journal.pone.0000290.

69. Sciamanna I, Gualtieri A, Cossetti C, Osimo EF, Ferracin M, Macchia G, Aricò E, Prosseda G, Vitullo P, Misteli T, Spadafora C. A tumor-promoting mechanism mediated by retrotransposon-encoded reverse transcriptase is active in human transformed cell lines. *Oncotarget*. 2013;4:2271–2287. doi: 10.18632/oncotarget.1403.

70. Oricchio E, Sciamanna I, Beraldi R, Tolstonog GV, Schumann GG, Spadafora C. Distinct roles for LINE-1 and HERV-K retroelements in cell proliferation, differentiation and tumor progression. *Oncogene*. 2007;26:4226–4233. doi: 10.1038/sj.onc.1210214.

71. Kabeya Y, Mizushima N, Yamamoto A, Oshitani-Okamoto S, Ohsumi Y, Yoshimori T. LC3, GABARAP and GATE16 localize to autophagosomal membrane depending on form-II formation. *J Cell Sci*. 2004;117(pt 13):2805–2812. doi: 10.1242/jcs.01131.

72. Mizushima N. The pleiotropic role of autophagy: from protein metabolism to bactericide. *Cell Death Differ*. 2005;12(suppl 2):1535–1541. doi: 10.1038/sj.cdd.4401728.

73. Smyth SS, McEver RP, Weyrich AS, Morrell CN, Hoffman MR, Arepally GM, French PA, Dauerman HL, Becker RC; 2009 Platelet Colloquium Participants. Platelet functions beyond hemostasis. *J Thromb Haemost*. 2009;7:1759–1766. doi: 10.1111/j.1538-7836.2009.03586.x.

74. Vachiat A, McCutcheon K, Tsabedze N, Zachariah D, Manga P. HIV and ischemic heart disease. *J Am Coll Cardiol*. 2017;69:73–82. doi: 10.1016/j.jacc.2016.09.979.

75. Funderburg NT, Lederman MM. Coagulation and morbidity in treated HIV infection. *Thromb Res*. 2014;133(suppl 1):S21–S24. doi: 10.1016/j.thromres.2014.03.012.

76. Tenorio AR, Zheng Y, Bosch RJ, Krishnan S, Rodriguez B, Hunt PW, Plants J, Seth A, Wilson CC, Deeks SG, Lederman MM, Landay AL. Soluble markers of inflammation and coagulation but not T-cell activation predict non-AIDS-defining morbid events during suppressive antiretroviral treatment. *J Infect Dis*. 2014;210:1248–1259. doi: 10.1093/infdis/jiu254.

77. Younas M, Psomas C, Reynes J, Corbeau P. Immune activation in the course of HIV-1 infection: Causes, phenotypes and persistence under therapy. *HIV Med*. 2016;17:89–105. doi: 10.1111/hiv.12310.

78. Auerbach E, Aboulafia DM. Venous and arterial thromboembolic complications associated with HIV infection and highly active anti-retroviral therapy. *Semin Thromb Hemost*. 2012;38:830–838. doi: 10.1055/s-0032-1328887.

79. Pittoggi C, Sciamanna I, Mattei E, Beraldi R, Lobascio AM, Mai A, Quaglia MG, Lorenzini R, Spadafora C. Role of endogenous reverse transcriptase in murine early embryo development. *Mol Reprod Dev*. 2003;66:225–236. doi: 10.1002/mrd.10349.

80. Dai L, Huang Q, Boeke JD. Effect of reverse transcriptase inhibitors on LINE-1 and Ty1 reverse transcriptase activities and on LINE-1 retrotransposition. *BMC Biochem*. 2011;12:18. doi: 10.1186/1471-2091-12-18.

81. Sciamanna I, De Luca C, Spadafora C. The reverse transcriptase encoded by LINE-1 retrotransposons in the genesis, progression, and therapy of cancer. *Front Chem*. 2016;4:6. doi: 10.3389/fchem.2016.00006.

82. Xiao-Jie L, Hui-Ying X, Qi X, Jiang X, Shi-Jie M. LINE-1 in cancer: multifaceted functions and potential clinical implications. *Genet Med*. 2016;18:431–439. doi: 10.1038/gim.2015.119.

Highlights

- LINE-1 (long interspersed nuclear element-1) elements are one source of endogenous reverse transcriptase activity.
- Presence and function of endogenous reverse transcriptase activity and LINE-1 in human platelets has not previously been determined.
- LINE-1 retrotransposon reverse transcriptase activity reverse transcribes select mRNAs, inducing RNA–DNA hybrids.
- Inhibition of reverse transcriptase activity regulates platelet activation, thrombosis, and RNA–DNA hybrid formation which is a new mechanism of translational control.